

NANOCRYSTALLIZATION OF DAPSONE; A NOVEL APPROACH TO BOOST SOLUBILITY, DISSOLUTION, AND *IN-VITRO* ANTI-INFLAMMATORY ACTIVITY

Hanaa Mohammed Mostafa¹, Shaaban K. Osman², Gamal Zayed^{2,3*}

¹Pharmacist at Al-Azhar University Hospital, Assiut 71524, Egypt.

²Department of Pharmaceutics and Pharmaceutical Technology, Faculty of Pharmacy, Al-Azhar University, Assiut 71524, Egypt.

³Al-Azhar Center of Nanosciences and Applications (ACNA), Al-Azhar University, Assiut 71524, Egypt.

*Corresponding author e-mail: gamalzayed@azhar.edu.eg

ABSTRACT

The low aqueous solubility of dapsone (DPS), a widely used anti-acne drug, greatly limits its biological efficacy, especially the anti-inflammatory effect. This article has applied the nanocrystallization technique to increase the surface area which consequently improves the solubility, dissolution, and anti-inflammatory effect of dapsone. Span-stabilized dapsone nanocrystals (DPS-NCs) have been prepared using solvent-antisolvent crystallization technique. The obtained nanocrystals (NCs) were characterized by FTIR, DSC, and X-ray. The morphology, particles surface, sizes, and surface charge of DPS-NCs were examined by TEM, SEM, and zetasizer, respectively. Additionally, the *in vitro* solubility, dissolution, and anti-inflammatory of the DPS-NCs were investigated. DPS-NCs were spherical in shape with smooth surfaces and had a hydrodynamic particle size of about 149 ± 4.73 nm. The saturated aqueous solubility of DPS-NCs was 1.8 ± 0.05 mg/mL which was about 6 fold higher than that of a pure drug and showed improved *in vitro* dissolution. The used excipients did not interact chemically with the drug as indicated by DSC and FTIR. X-ray diffraction and TEM imaging confirmed that the produced nanocrystals (NCs) still have a certain degree of crystallinity and did not completely convert to the amorphous state. The *in vitro* anti-inflammatory of DPS-NCs greatly improved compared to pure drug. DPS-NCs could be considered a novel, promising, and effective therapeutic option for the treatment of acne as well as for relieving the accompanying inflammation.

Keywords: Dapsone nanocrystal, solvent-antisolvent, solubility, dissolutions, *in vitro* anti-inflammatory.

1. Introduction

Acne vulgaris is a common skin disorder that affects most people during the adolescence stage. The disease frequently affects regions of higher sebaceous glands such as the face, upper back, and anterior trunk. As the disease affects the exposed parts of the body, mainly the face, the affected patients may suffer from psychosocial disorders such as anxiety, depression, insomnia, and hyperactivity (**Toyoda and Morohashi 2001**). Pathologically, sebaceous glands secrete excessive sebum which is later infected by acne-causing microorganisms, Propionibacterium acne (P. acne) (**Xu and Li 2019**). After that, the bacteria colonized, grow, and secrete certain enzymes such as proteases, lipases, and hyaluronidases which potentiate and augment skin inflammation and hyperkeratinization around pilosebaceous units (**Shalita and et al. 2011; Berson and Shalita 1995**). According to the degree of inflammation, acne lesions are classified as inflammatory and non-inflammatory. Non-inflammatory acne is characterized by open or closed comedones while inflammatory lesions are diagnosed by two types of papules. The first one is characterized by raised erythematous lesions while the other inflammatory type is characterized by collections of white pus at the surface. Once comedones rupture they release their contents into the skin's surface and the inflammatory response is potentiated. The successful and effective treatments of the disease improve all of these abnormalities and additionally resolve psychological issues (**Alston and et al. 2022; Brown and Food And Drug Administration 2014**).

Dapsone (DPS), a sulfone derivatives antibiotic, is a relatively new anti-acne drug that has been shown to possess antibacterial and anti-inflammatory effects and has been approved by the FDA, in 2005, for the treatment of acne vulgaris. Its antimicrobial activity contributed to anti-folate by competing with para-aminobenzoic acid for the active site of dihydropteroate synthetase. The antimicrobial spectrums of the drug included *in vitro* antibacterial against Propionibacterium acnes which was commonly detected bacteria in acne lesions. However, other bacteria such as Staphylococcus epidermis (S. epidermis) had been reported to be affected by dapsone (**Schneider-Rauber and et al. 2020**). The *in vivo* anti-inflammatory effect of the drug was attributed to the inhibition of elastase enzymes, leukocyte peroxidase, and chemotaxis (**Wozel and Blasum 2014**).

According to the Biopharmaceutic Classification System (BCS), DPS is a class II drug with low solubility and high permeability ($\log P = 0.97$) and according to USP, its aqueous solubility is very slightly soluble (**Bergström et al. 2014**). The drug's low therapeutic index and significant microbiological resistance were linked to its low solubility. Enhancing and improving the low aqueous solubility were considered major challenges encountered with the development of new pharmaceutical formulations to achieve optimum therapeutic effects (**Nyamba et al. 2021**).

Physical and chemical alterations of medications, as well as additional approaches such as particle size reduction, crystal engineering, salt formation, solid dispersion, and complexation, were used to improve the solubility of poorly water soluble drugs (**Gao et al. 2012**). Nanocrystals (10-200 nm) preparation is one of the newest physical strategies to improve the dissolution rate of poorly water-soluble materials. According to the Noyes-Whitney equation, the particle size reduction will result in an increased surface area to

volume ratio which increases the solubility and dissolution rate of badly soluble drugs (Chen et al. 2011). Improvement of the solubility of low soluble highly permeable molecules will subsequently enhance the bioavailability and efficacy of such drugs (Merisko-Liversidge and Liversidge 2008).

Typically, nanoparticles are prepared using the either top-down or bottom-up method. In the top-down technique mechanical comminution, using a high energy mill, of larger particles into small nanoparticles is performed. This method requires high energy input, time-consuming, and also may induce contamination. While in the bottom-up approach nanoparticles are precipitated from the dissolved drug molecules. This method gives better product output by producing a homogeneous particle distribution with less energy input. Also, it utilizes inexpensive equipment (cost-effective) and takes place at ambient temperatures and atmospheric pressure which preserve the stability of processed materials (Abid et al. 2022). Production of stable nanoparticles requires coating of the particle's surface by a suitable stabilizer which prevents particle growth and/or aggregation during preparation and/or storage and also aids in the improvement of solubility and dissolution (Alshweiat et al. 2018; El-Feky et al. 2013).

Pharmaceutical researchers had developed many formulations to increase the solubility and bioavailability of dapsone. For example, nanostructured lipid carriers (composed of solid lipids and liquid lipids stabilized by surfactants), vesicles (niosomes, invasomes, and bilosomes), and micro-emulsion had been also prepared. All of these formulations contained multiple stabilizers, excipients, and have been prepared using several organic solvents which may be harmful to the human body (Schneider-Rauber et al. 2020; Bawazeer et al. 2020).

The main aim of the current work was the preparation of stable dapsone nanocrystals (DPS-NC) by reducing particle size and increasing surface area to enhance the drug solubility and dissolution without using harmful organic solvents and large number of stabilizers and/or different excipients. Span-stabilized nanoparticles were prepared by solvent anti-solvent technique using acetone as solvent and water as anti-solvent. The produced nanocrystals were characterized concerning particle size, surface charge, shape, surface roughness, solubility, *in vitro* dissolution and short-term dispersion stability. The interaction between the drug and the used excipients during the preparation of nanocrystals was investigated by FTIR, DSC, and X-ray. Finally, the *in vitro* anti-inflammatory of the produced nanocrystals was studied.

2. Materials and Methods

2.1. Materials

Dapsone (batch number 289/5/19 and EX. Date 2/24) was purchased from El-Nile Co., El-Swah square-America, Cairo, Egypt. Sorbitan mono-oleate (Span 80) was purchased from Sigma-Aldrich Chemical Co. St. Louis MO (USA). Acetone, methanol, and other used chemicals were of analytical grade and were used as received. Blood samples were obtained from blood donors at the Blood Bank of Al Azhar University Hospital in Assiut, Egypt. Ethical approval ZA-AS/PH/7/C/2022

2.2. Methods

2.2.1. Preparation of Dapsone Nanoparticles

Dapsone nanoparticles (NPs) were produced by solvent anti-solvent precipitation method using water as anti-solvent, acetone as a solvent, and Span 80 as a surface stabilizer. The required amounts of pure drug and Span 80, as presented in Table 1, were dissolved in 5 mL of acetone (water miscible organic solvent) in a test tube under sonication for 3 minutes at room temperature until a clear organic solution was obtained. The produced organic solution was then slowly dropped (1 mL/3 minutes) into 50 mL of pure water using a plastic syringe over 15 minutes under continuous stirring at room temperature using an overhead magnetic stirrer (Daihan Scientific Co., Korea) adjusted at 1000 rpm. After that, the aqueous phase was continuously stirred for additional 2 hrs to ensure complete evaporation of the organic solvent which was detected by the absence of acetone odour. To obtain pure NPs, the produced nanosuspension was centrifuged, using high speed centrifuge (Mumbai, India), at 10000 rpm for 30 minutes. The supernatant was discarded, and the precipitated nanoparticles were washed twice with distilled water and oven vacuum dried (Zeamil Horyzont Co., Poland) at 50° C for one day until constant weight to ensure complete removal of water and acetone. The dried nanoparticles were placed in airtight glass containers and stored in a desiccator till further use. The actual compositions of the different formulations of the prepared nanoparticles were listed in table 1 (Sinha and et al. 2022; Ibrahim et al. 2019).

Table (1): Composition of the prepared dapsone nanoparticles using Span 80 as a stabilizer

| Formula Code | Ingredients | | | | |
|--------------|--------------|--------------|-----------------------------|--------------|------------|
| | Dapsone (mg) | Span 80 (mg) | Dapsone/Span 80 Ratio (W/W) | Acetone (mL) | Water (mL) |
| F1 | 100 | 65 | 1.54 | 5 | 50 |
| F2 | 100 | 45 | 2.22 | 5 | 50 |
| F3 | 100 | 25 | 4 | 5 | 50 |
| F4 | 75 | 65 | 1.15 | 5 | 50 |
| F5 | 75 | 45 | 1.67 | 5 | 50 |
| F6 | 75 | 25 | 3 | 5 | 50 |
| F7 | 50 | 65 | 0.77 | 5 | 50 |
| F8 | 50 | 45 | 1.11 | 5 | 50 |
| F9 | 50 | 25 | 2 | 5 | 50 |

2.2.2. Determination of Saturation Solubility

Saturation solubility of materials depends mainly on the temperature and the properties of the dissolution medium. However, below a size of approximately 1-2 μm , the saturation solubility is also a function of particle size (Ashok Kumar et al. 2015).

The saturation solubility of pure drug, physical mixture, and Span stabilized nanoparticles were determined in phosphate buffer (pH, 6.8). Excess amount of each sample was added to 10 mL of the buffer in screw glass tubes which were shaken at 50 rpm in a thermostatically controlled water bath shaker kept at 37 °C for 48 hrs. At the end of the specified time, samples were centrifuged at 10000 rpm at 4 °C and the absorbance of the drug in supernatants was then analyzed spectrophotometrically (Shimadzu Co., Japan) at λ_{max} 291 nm to quantitatively determine the amount of soluble drug per mL of buffer solution. All the experiments were carried out in triplicate (Agrawal et al. 2004).

2.2.3. Characterization of the Prepared Nanoparticles

2.2.3.1. Fourier Transformer Infrared Spectroscopy (FTIR)

This experiment was carried out to detect any possible interaction between the drug and the used stabilizer during the preparation of nanoparticles. Five mg of the pure drug, Span 80, and the equivalent weight of selected nanoparticles were finely crushed and mixed with KBr separately and compressed into disc which were scanned in the spectral region from 4000 to 400 cm^{-1} (FT-IR spectrophotometer Shimadzu, Corporation, Japan) (Zhao et al. 2014).

2.2.3.2. Differential Scanning Calorimetry (DSC)

Thermal analysis was used to estimate the chemical and physical changes such as drug crystallinity of the drug upon size decrease by the nanosizing process. Five mg of pure drug and selected nanoparticles were placed in standard aluminum pans with a lid. Pans containing the samples were heated from 20 to 300 °C at a heating rate of 10 °C /min under nitrogen flow rate of 25 mL/min. (DSC-50, Shimadzu Co., Japan) (Altamimi and Neau 2016).

2.2.3.3. Powder X-ray Diffraction (PXRD)

The crystallinity of pure dapsone and dapsone nanoparticles were evaluated by PXRD. Powder X-ray diffraction patterns (diffractograms) of the selected nanoparticles and pure drug were obtained by X-ray diffractometer (Model PW 1710 control unit Philips, anode material Cu 40 K.V, 30 M.A, Philips, Germany). Each sample was scanned in the two theta degree (2θ) range of 4 to 60 with a step size of one degree at a scan rate of 0.06/s (Medarević et al. 2020).

2.2.3.4. Scanning Electron Microscopy (SEM)

The surface morphological features of the selected dapsone nanoparticles were examined by scanning electron microscopy (SEM) (JSM-5400LVSEM, Jeol, Japan). A vacuum-dried samples of nanosuspension was placed on a metal grid coated with gold-palladium followed by an examination at suitable required magnifications (Khan et al. 2019).

2.2.3.5. Transmission Electron Microscopy (TEM)

The morphology and the size of the drug's nanoparticles were determined by high-resolution electron microscopy (TEM). One drop of freshly prepared nanoparticles was placed on the carbon-coated copper grid and left to dry. After drying, the samples were imaged by TEM at magnifications of 5000-20,000 using (FEI Tecnai G2 Field Emission Gun, HR-TEM operating at 200 kV) (Alves et al. 2021).

2.2.3.6. Particle Size, PDI and Zeta Potential Measurements

The hydrodynamic size, PDI and zeta potentials of all nanoparticles preparation were measured immediately after producing the formulae by dynamic laser light scattering using zetasizer ZS 90 (Malvern, England). About 3 mL of each prepared nanoparticles were properly diluted and the size and PDI of each sample were measured at 25 °C, measurements were carried out in triplicate for each sample (Shariare et al. 2018).

2.2.3.7. Determination of the Production Efficiency (PE)

Dapsone nanoparticle production efficiency (PE) was determined by dissolving a known amount of completely dried nanoparticles powder (5 mg) in methanol and diluted with phosphate buffer (pH 6.8). The absorbance of each sample was measured spectrophotometrically (Shimadzu Co., Japan) at λ_{\max} 291 nm and the corresponding drug weight was calculated using a standard calibration curve of pure drug constructed under the same conditions. The production efficiency of dapsone nanocrystals was calculated using equation 1 (Mothilal et al. 2014).

$$\text{PE \%} = \frac{\text{Weight of dapsone in nanocrystals}}{\text{Total weight of nanocrystals}} \times 100 \quad \text{equation (1)}$$

2.2.3.8. *In vitro* Dissolution Studies

The *in vitro* dissolution profiles of raw dapsone and 9 prepared nanoparticles batches were performed using USP dissolution apparatus type II (Dissolution test apparatus, SR II, 6 flasks, paddle type, Hanson research Co., USA). Accurately weighed 10 mg of pure drug and the equivalent amount of all prepared nano formulae were dispersed in 900 mL of phosphate buffer (pH 6.8) which was stirred at 100 rpm and maintained at 37 ± 1 °C for 2 hrs. At specified time intervals, 10, 15, 20, 25, 30, 45, 60, 90, and 120 minutes, 5 mL samples were withdrawn, filtered using filter tip, and replaced immediately with an equal volume of fresh dissolution medium to maintain the dissolution volume constant. The absorbance of the collected samples was determined by UV-vis spectrophotometry (Shimadzu 1601, Japan) at λ_{\max} 291 nm, the specific λ_{\max} of the drug. The concentration of the drug in each sample was calculated using a standard calibration curve of the drug and the percentage of drug dissolved was calculated. Each dissolution experiment was done in a triplicate pattern and represented graphically as the cumulative percent drug dissolved with time (Gamal Zayed 2014).

2.2.3.9. Dispersion Stability of the Prepared Nanoparticles

The selected batch was subjected to a short-term dispersion stability test. Freshly prepared samples were stored in 5 mL sealed glass vials for three months. The stored samples were exposed to varying conditions of temperature and relative humidity at 25 °C/65% RH and 4 °C/65 % RH for three months in humidity controlled oven. The stored samples were periodically inspected for any sedimentation or changes in their physical appearance and evaluated with respect to particle size and PDI at the interval of zero, one month, two months, and third months respectively (He et al. 2017).

2.2.3.10. Investigation of the *In vitro* Anti-inflammatory Activities.

The *in vitro* anti-inflammatory activity of the prepared dapson nanoparticles were tested using the recently reported methods, inhibition of albumin denaturation, and membrane stabilization methods.

2.2.3.10.1: Inhibition of Albumin Denaturation.

Albumin denaturation is the main cause of inflammation which is characterized by swelling redness and pain in the affected area. Non-steroidal anti-inflammatory drugs (NSAIDs) act by binding to plasma albumin and preventing the denaturation and the consequent swelling redness and pain (Saso et al. 2001).

2 mL containing varying concentrations (500, 400, 300, 200,100, and 50 µg/mL) of the selected formula of dapson nanocrystal, 2.8 mL of PBS (pH 6.8), and 0.2 mL of 5% egg albumin were mixed together and incubated in a water bath at 37 °C for 20 minutes and then heated at 70 °C for 5 minutes. Equal concentrations of pure dapson suspensions were used for comparison. The absorbance of each sample was measured spectrophotometrically at 660 nm using phosphate buffer as a blank. Each experiment was carried out in triplicates and the percentage inhibition of albumin denaturation was calculated applying equation 2 (Bailey-shaw et al. 2017).

$$\% \text{ Inhibition of albumin denaturation} = \left(\frac{\text{Abs. Control} - \text{Abs. Sample}}{\text{Abs. control}} \right) \times 100 \quad \text{equation (2)}$$

2.2.3.10.2. Human Red Blood Cell (HRBC) Membrane Stabilization Methods.

Usually, the lysosomal enzymes are released during inflammation and produce multiple disorders related to chronic or acute inflammation. The anti-inflammatory drugs act either by stabilizing the lysosomal membrane or inhibiting these lysosomal enzymes. Due to the similarity between the membrane of red blood cells and the lysosomal membrane, many studies were used to check the stability of the HRBC membrane as an indicator of the anti-inflammatory effect (Gunathilake and et al. 2018a).

Preparation of human red blood cell suspension.

Fresh blood was collected, in heparinized tubes, from a healthy volunteer who had not received any non-steroidal anti-inflammatory drugs two weeks before the experiment. Blood containing tubes were centrifuged at 2500 rpm for 10 minutes to separate plasma

from RBCs and the plasma was discarded. HRBCs were washed with 0.9% normal saline and the volume of blood was reconstituted with isotonic 0.9% normal saline to 10% (v/v) suspension and the *in vitro* anti-inflammatory effect of dapsone nanocrystals was investigated by two methods. The experiment was conducted according to guidelines of the Institutional Ethical Committee of the faculty of pharmacy, Al-Azhar University at Assiut, Egypt (ethical approval number; ZA-AS/PH/7/C/2022) (**Gunathilake and et al. 2018b**).

2.2.3.10.2.1. Heat-induced hemolysis

1 mL of varying concentrations of DPS-NC or pure dapsone suspension (500, 400, 300, 200, 100, and 50 $\mu\text{g/mL}$) was added to 1 mL of 10% HRBCs suspension test tubes. Control samples were prepared by adding 1 mL of 10% HRBCs suspension to 1 mL of distilled water. The tubes were incubated at 55 °C for 30 minutes in a thermostatically controlled water bath, then tubes were cooled to room temperature, centrifuged at 3000 rpm for 5 minutes and the absorbance of the supernatant was measured at 560 nm. Each experiment was done in triplicates and the percentage inhibition of hemolysis (the hemoglobin content in the supernatant) was calculated according to equation 3 (**Xiao et al. 2021**).

$$\% \text{ Hemolysis inhibition} = \left(\frac{\text{Abs Control} - \text{Abs Sample}}{\text{Abs control}} \right) \times 100 \quad \text{equation (3)}$$

2.2.3.10.2.2: Hypotonicity-induced hemolysis

1 mL phosphate buffer (pH 7.4) containing varying concentrations of pure dapsone suspension or dapsone nanoparticle was added to 2 mL hyposaline solution (0.36% NaCl in water) and finally added to 0.5 mL 10 % HRBCs suspension. In the control experiment, distilled water was used instead of a drug. The mixture was incubated at 37 °C for 30 minutes, then centrifuged at 3000 rpm for 20 minutes and the absorbance of the supernatant was measured at 560 nm. The experiment was done in triplicates and the percentage inhibition of hemolysis (the hemoglobin content) was calculated using equation 3 (**Umapathy et al. 2010**).

3. Results

3.1. Formation of Stable Nanocrystals

Solvent anti-solvent precipitation is a simple approach commonly used to modify the size of poorly water-soluble drugs. Acetone was used, specifically, as a solvent for several basic reasons; it has the ability to solubilize large amount of both DPS and Span 80, completely miscible with water (anti-solvent of the drug) and it is rapidly evaporated at low temperatures (**Li et al. 2019**). Moreover, the term stabilizer refers to hydrophobic surfactant (Span 80) which was used in our study. The used stabilizer has a good affinity to drug particles, wet it with a fast diffusion rate, and effectively adsorbed on the surface of drug particles in the water solvent mixture. The effective adsorption of Span 80 on the particle's surfaces acquired the nanocrystal sufficient stability and prevented the crystal growth by steric stabilization. The applied method depended on the generation of ultrafine crystals upon the slow addition of an organic solution into water (anti-solvent) under rapid

mixing at a stirrer at 1000 rpm at room temperature. The process of nanocrystallization was done through two phases, nucleation (nuclei generation) and crystal growth. During the crystal growth phase, the production of stable suspension is challenging, especially, with a high nucleation rate and formation of small-sized nanocrystals with high surface area. Large surface area nanocrystals are acutely thermodynamically unstable and may result in crystal agglomeration to decrease their surface energy. To prevent and arrest nanocrystals growth, as a consequence of larger surface area and thermodynamic instability, Span 80 (non-ionic surfactant), as a surface stabilizer, with high affinity to the particle's surface, had been added during the process of nanocrystal formation which gave the effective steric barrier against crystals growth and aggregation (Wang et al. 2013).

3.2. Saturation Solubility

The saturation solubility of pure dapson, physical mixture, and DPS-NC are shown in figure 1. The solubility of the pure drug and physical mixture was found to be $297 \pm 3.5 \mu\text{g/mL}$ and $314 \pm 2.7 \mu\text{g/mL}$, respectively, which demonstrate the very poor aqueous solubility of the drug. In contrast, the solubility of Span stabilized DPS-NC was found to be $1800 \pm 50 \mu\text{g/mL}$ which is about 6 folds higher than that of the pure drug. These results indicated that the nanocrystallization of dapson in water in the presence of surface active agent, Span 80, could be an effective physical technique to increase the aqueous solubility of the drug (Junyaprasert and Morakul 2015).

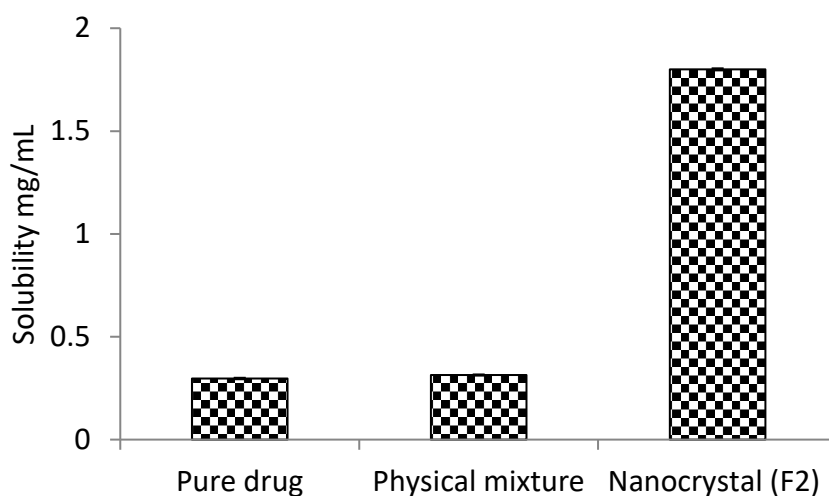


Figure (1): Saturation solubility of pure dapson, physical mixture and dapson nanocrystal at 37 °C in phosphate buffer pH (6.8).

3.3. Fourier Transformer Infrared Spectroscopy (FTIR)

FTIR spectra reported in study confirmed that there was no major shifting as well as no loss of functional peaks between the spectra of pure dapson and nanocrystals. The spectrum of DPS-NC only showed low intensity bands probably due to the dilution of the drug by the adsorbed stabilizer. FTIR spectra of DPS and nanosized DPS-NC were shown in figure 2. We can observe as a characteristic transmission bands at 3300 cm^{-1} and 3456 cm^{-1} corresponding to the stretching of the amine group (N-H) and peaks corresponding

to bending vibration of -NH_2 groups between 1590 and 1550 cm^{-1} . The bands located at 1143 cm^{-1} and 1180 cm^{-1} were corresponding to the symmetric and asymmetric vibrations of the sulfone group (O=S=O). These finding demonstrated the absence of intermolecular interaction or changes in the chemical structure of the drug during or after the nanoprecipitation process (Chaves et al. 2015).

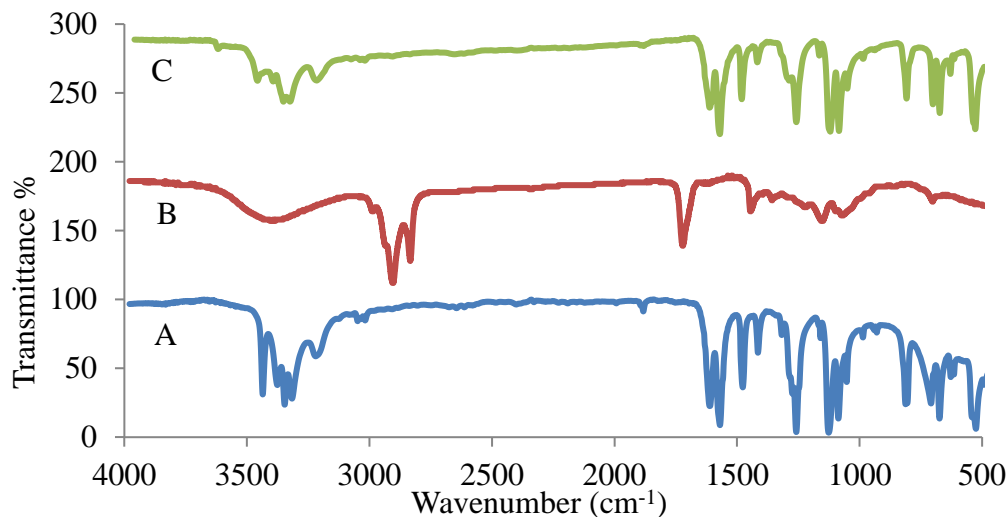


Figure (2): FTIR spectra of pure drug (A), Span 80 (B) and nanocrystals (C).

3.4. Differential Scanning Calorimetry (DSC)

DSC is widely used to evaluate the crystalline or amorphous nature of the drug within the obtained formulation and may detect any possible interactions with other ingredients. Figure 3 shows the DSC thermograms of pure dapsone and selected nanocrystals formulae, small one. Pure drug revealed an intense sharp endothermic peak at $180\text{ }^\circ\text{C}$ corresponding to drug melting with fusion enthalpy equal to -121.81 J/g . While nanocrystals, thermogram showed a melting endothermic peak at $178\text{ }^\circ\text{C}$ with fusion enthalpy equal to -25.04 J/g . The results of the thermal analysis proved the chemical integrity of the drug after nanocrystallization because both pure drug and nanocrystal showed nearly the same melting peaks. The lower melting intensity of the endothermic peak of DPS-NC as indicated in figure 3 could be attributed to the smaller particle size of the drug nanocrystal (Khan et al. 2020).

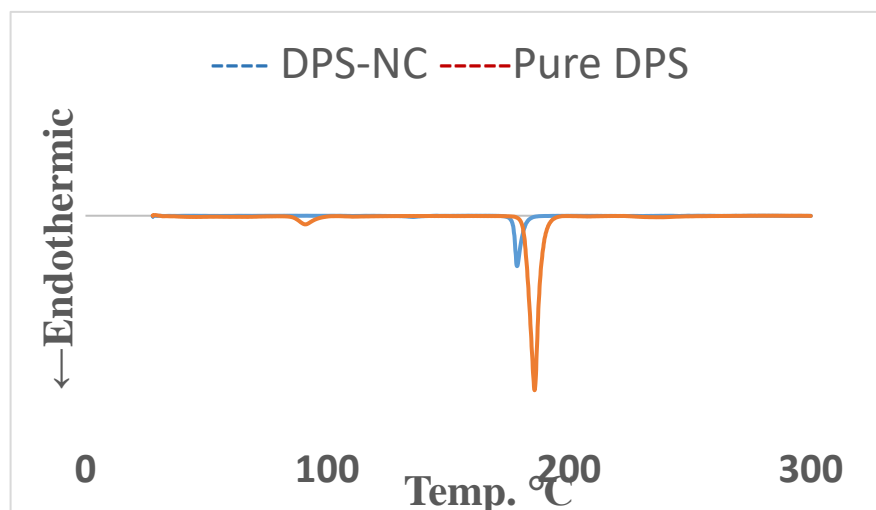


Figure (3): DSC thermograms of pure drug (orange curve) and nanocrystal (blue curve).

3.5. Powder X-ray diffraction (PXRD)

The XRD diffraction pattern of pure dapstone showed sharp intense peaks at 2θ 13.10°, 16.99°, 17.84°, 19.35°, 20.86°, 22.46°, 23.73° and 29.10° indicating the high crystalline nature of the drug as presented in figure 4. Compared to the characteristic peak positions of pure drug, there was no difference in the positions of the characteristic peaks of selected nanocrystals. The only detected difference was in the peaks intensity, which may be attributed to particle size reduction and presence of the stabilizer at the crystal surfaces. Usually, drugs with lower crystallinity and smaller size induce improvement of dissolution rate, harvesting higher saturation solubility and oral bioavailability than pure crystalline materials presented in figure 4. However, the maintenance of the original crystalline structure of any drug is required for long-term stability because of its low energy state (He et al. 2017).

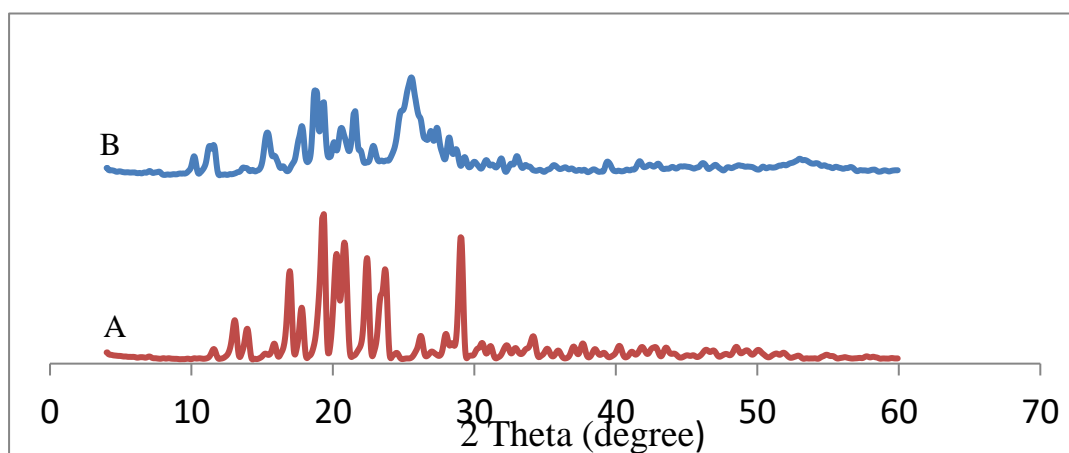


Figure (4): X-ray diffraction patterns of pure drug (A) and nanocrystal (B).

3.6. Scanning electron microscopy (SEM)

The SEM images of dapsons nanocrystals were displayed in figure 5. SEM investigation indicated that Span coated DPS-NCs produced by solvent-antisolvent precipitation were very small in size with spherical shapes, smooth surfaces, and definite edges. SEM images didn't show any aggregations of particles and nanocrystals still in the nanometer even after complete drying and solidification. There is also a previous study that indicated that small spherical particles have a higher dissolution rate than large, irregular particles (Mosharraf and Nyström 1995).

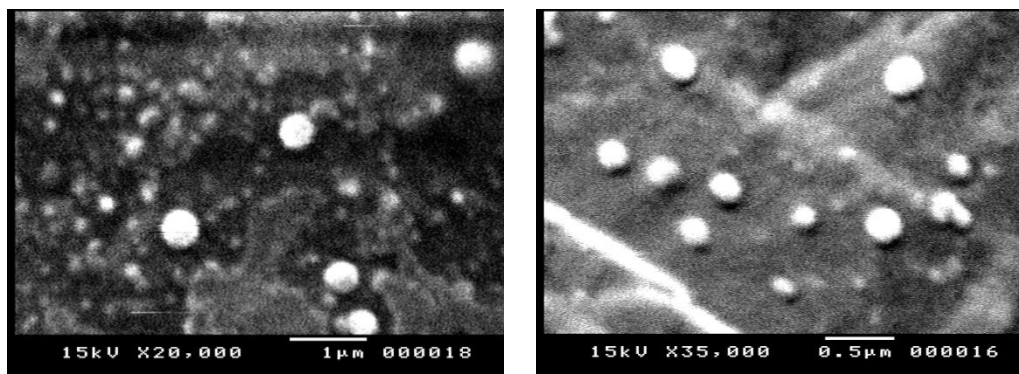


Figure (5): Scanning electron microscope images of dapsons nanocrystal (F2)

3.7. Transmission Electron Microscopy (TEM)

TEM image of the prepared nanocrystal was shown in figure 6. The nanocrystal appears under a high-resolution electron microscope (TEM) as uniform spherical particles within the nanometer range of less than 100 nm. There is a large difference between the sizes measured by DLS and the sizes determined by TEM. The smaller size of nanocrystal measured by TEM could be due to the fact that zetasizer measuring the hydrodynamic sizes of particles i.e the size of particles with the surrounding moving layer of the dispersion medium but TEM measured only the actual size of dried nanocrystal so gives images with a smaller particle size compared to that of DLS result.

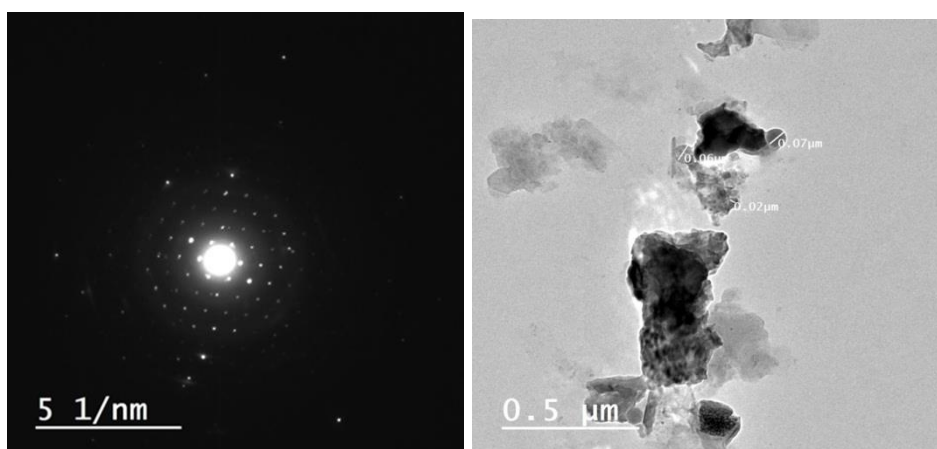


Figure (6): TEM photographs of dapsons nanocrystal.

3.8. Particle size, PDI and Surface Charge

The most important parameters for characterization the prepared nanocrystals were particle size, polydispersity index (PDI) and surface charge (zeta potential). Particle size is a reflective mirror for physicochemical properties such as physical stability, dissolution pattern, saturation solubility, and bioavailability. Small sized Span coated DPS-NC were obtained where the particle sizes ranged from 149.07 ± 4.73 nm to 252.77 ± 7.94 nm with narrow size distribution as indicated by low polydispersity indexes (PDI) and presented in figure 7 and table 2. Particles having PDI less than 0.7 are considered monodisperse nanoparticles which mean that the sizes of individual particles are close to each other i.e there is no large difference in the size between the smaller particles and larger particles. So maintaining a narrow particle size distribution was the greatest challenge for ensuring the of stability nanosuspension. The PDI results of all 9 Span coated dapsons nanocrystals formulations were in the range of 0.084 to 0.299 which was considered a fair indication for the mono-size distribution of particles (table 2).

Table (2): Particle size, PDI, production efficiency (PE) and zeta potential of the prepared dapsons nanocrystals

| Formula Code | Average particle size (nm) | PDI | Zeta potential (mV) | PE (%) |
|--------------|----------------------------|----------------------|---------------------|-------------------|
| F1 | 252.76 ± 7.94 | 0.236667 ± 0.081 | -25.5 ± 1.8 | 96.4 ± 0.01 |
| F2 | 222.4 ± 5.79 | 0.177667 ± 0.026 | -39.6 ± 0.58 | 97.5 ± 0.025 |
| F3 | 149.07 ± 4.73 | 0.167 ± 0.098 | -30.2 ± 2.41 | 98.88 ± 0.02 |
| F4 | 244.5 ± 23.39 | 0.223 ± 0.033 | -20.7 ± 1.01 | 94.68 ± 0.020 |
| F5 | 199.97 ± 10.5 | 0.17 ± 0.035 | -37.1 ± 2.01 | 95.95 ± 0.032 |
| F6 | 160.53 ± 6.22 | 0.214667 ± 0.028 | -35.0 ± 1.73 | 96.87 ± 0.015 |
| F7 | 211.93 ± 29.77 | 0.249 ± 0.02 | -20.5 ± 3.31 | 92.5 ± 0.03 |
| F8 | 166 ± 12.60 | 0.299333 ± 0.170 | -25.4 ± 3.13 | 93.77 ± 0.025 |
| F9 | 193.6 ± 4.16 | 0.083667 ± 0.05 | -19.1 ± 3.8 | 95.08 ± 0.051 |

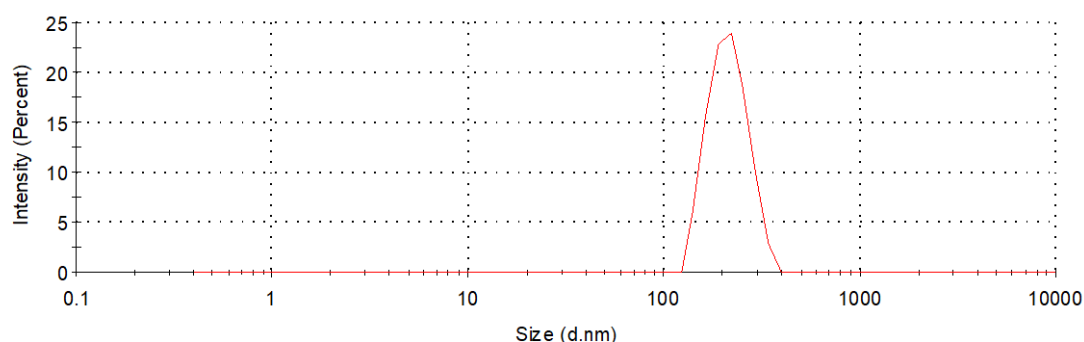


Figure (7): Hydrodynamic size distribution of the dapsons nanocrystal.

The zeta potential is a fundamental parameter for predicting nanocrystal dispersion stability as it measures electric charge on the surface of particles. It is well known that particles with zeta potential higher than 30 mV are characterized by high dispersion stability. In this case, the electrostatic repulsion between similarly charged nanoparticles is higher than the hydrophobic-hydrophobic interaction and consequently particles remain individually distributed within the dispersion medium. The observed zeta potential values for all dapsone nanocrystal formulations were in the range of -19.1 mV to -39.6 mV (table 2) which prove the helpful role of surface charge in nanocrystal stabilization.

3.9. Determination of the Production (Entrapment) Efficiency (PE)

The production efficiency (yield) of dapsone nanocrystals in each formula was determined using a spectrophotometer (Shimadzu Co., Japan) at λ_{\max} 291 nm to quantitatively determine the amount of the drug after vacuum oven drying and solidification. High production efficiencies, more 92%, were observed for the prepared formulae as presented in table 2.

3.10. *In vitro* dissolution studies

The dissolution rate of drug is one of the most important results for nanocrystals evaluation because the higher dissolution rate indicates successful improvement of dissolution and bioavailability. The dissolution profiles of pure dapsone and different dapsone nanocrystals were illustrated in figures 8, 9, and 10. According to the Noyes-Whitney equation, the dissolution rate is directly proportional to the surface area of solid particles subjected to the dissolution medium. The faster dissolution rates of the nanocrystals, especially within the first 25 minutes, could be attributed to small particle size and greater surface area in comparison with pure drug. The Nanocrystals formula of F6, F3, F2, F9, F8, F7, F4, F5, and F1 gave faster dissolution rates in descending order due to reduction in particle size and increased surface area. After 45 minutes F2 exhibited the highest dissolution over other tested nanocrystal formulae. Moreover, F2 showed the highest zeta potential and it considered to the most stable formulae. For these reasons, F2 was selected as the best formulae and was used to perform other all investigation in the study. Moreover, the surface coating of nanocrystals by a non-ionic stabilizer, Span 80 which is a water dispersible surfactant, accelerated the drug release and gives a higher impact on the enhancement of dissolution rate as shown in the drug release. F2 nanocrystal was found to exhibit the highest dissolution rate where 93.35 % of the drug was dissolved within 45 minutes compared to only 25.55 % for pure drug (figure 8). The highest dissolution rate of F2 is due to the smaller particle size, larger surface area, and using an intermediate concentration of Span 80.

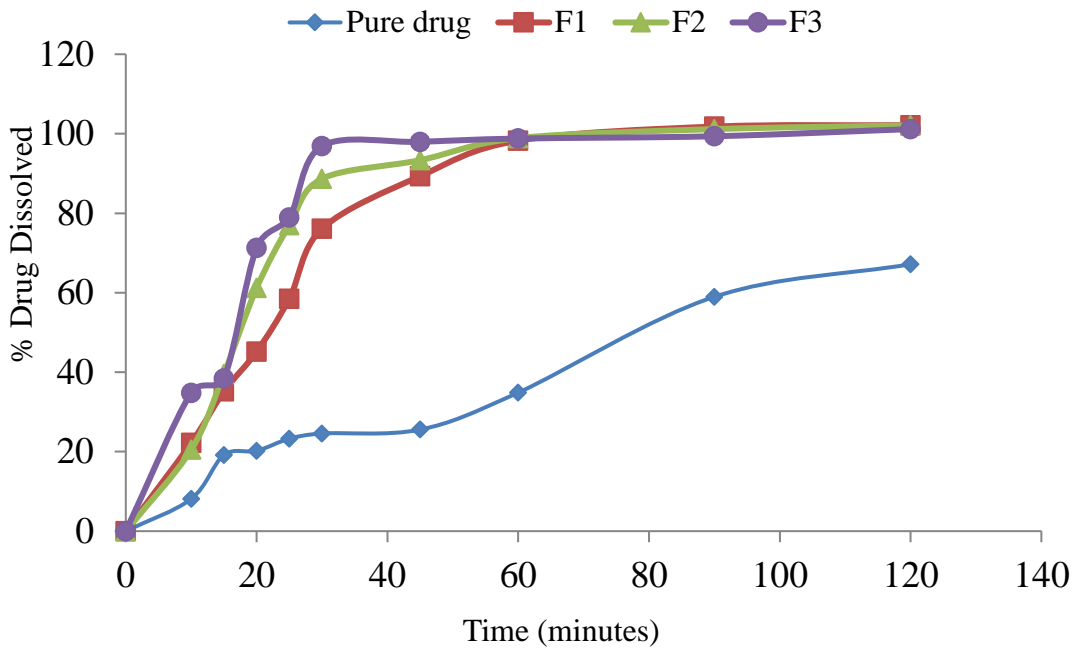


Figure (8): Dissolution profiles of pure drug, nanocrystal formulae F1, F2 and F3

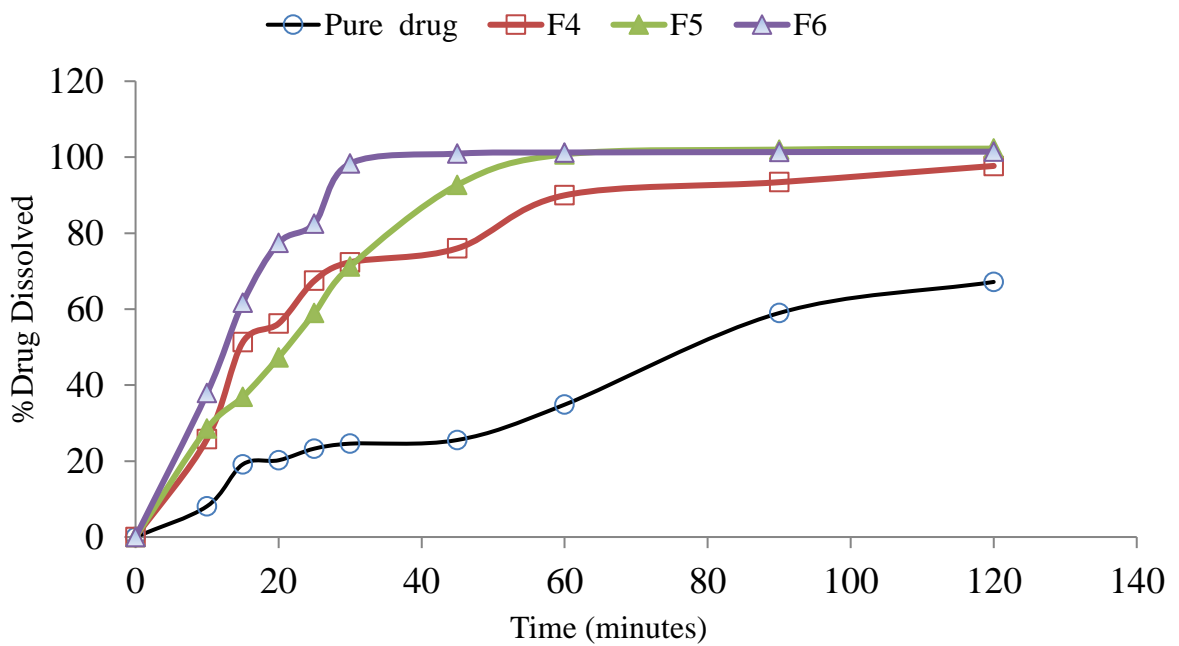


Figure (9): Dissolution profiles of pure drug, nanocrystal formulae F4, F5 and F6

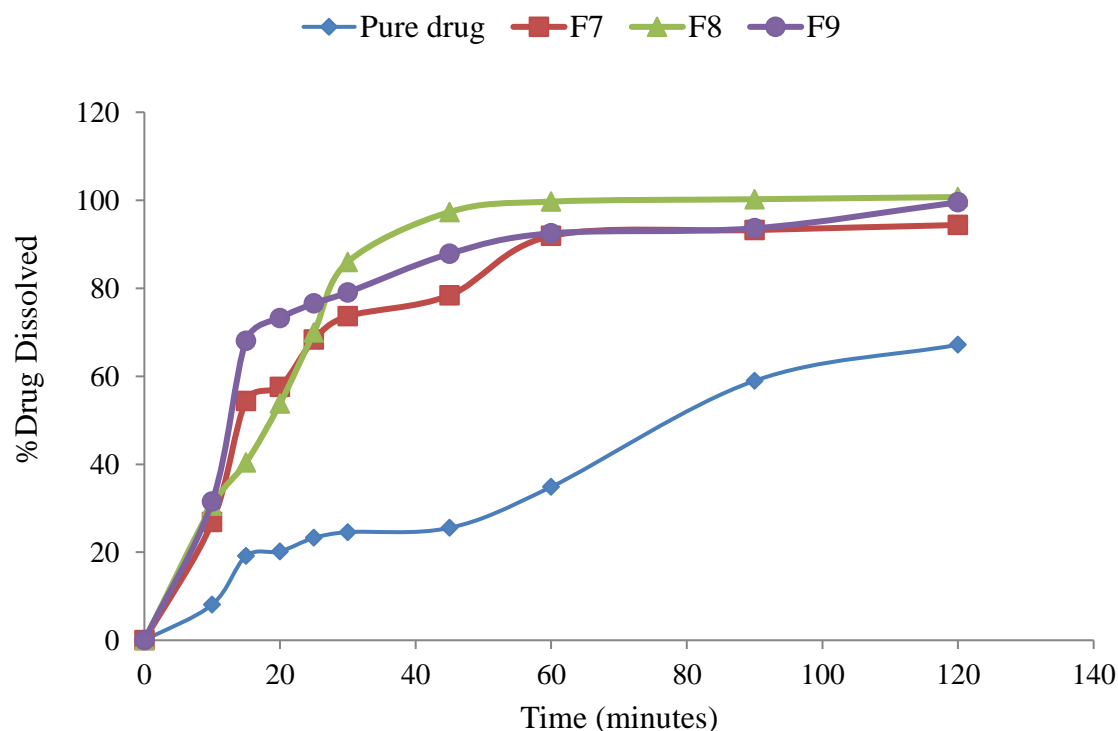


Figure (10): Dissolution profiles of pure drug, nanocrystal formulae F7, F8, and F9

3.11. Dispersion stability of dapsone nanocrystals

The stability data of the stored preparation at different storage conditions was shown in table (3) and figure 11. Sufficient steric repulsion occurs among the particles due to the type and amount of stabilizer provide high physical stability. Moreover, the homogeneous particle size of nanocrystals affects the physical stability of formulations because the poor homogeneity of particles causes the growth of larger particles (Ostwald ripening). That is why the appearance and physical characteristics did not change upon storage of particle dispersion for 3 months in the refrigerator at 4 °C/RH 65±5% for 3 months. But under the ambient conditions, a loose layer of sediment appeared in vials containing the NC. However, the sedimentation disappeared rapidly when the vials were shaken manually. Thus, the formulation stored at 4 °C/ RH 65±5% showed better stability if compared with the formulation stored at 25 °C/ RH 65±5%. Finally, the selected formula did not show any significant change in both parameters under different conditions. It indicates that this formulation was able to retain its stability for up to 3 months.

Table (3): Particle size and PDI of fresh and stored nanocrystal

| Parameter | Fresh samples | Stored at 4 °C | | | Stored at 25 °C | | |
|-----------|---------------|----------------|------------|--------------|-----------------|-------------|--------------|
| | | One month | Two months | Three months | One month | Two months | Three months |
| Size (nm) | 222.4±5.79 | 222.4±5.45 | 225.6±4.86 | 228.7±5.64 | 246±3.71 | 251.4±4.48 | 261.3±3.955 |
| PDI | 0.178±0.026 | 0.191±0.0251 | 0.2±0.0235 | 0.203±0.0211 | 0.233±0.022 | 0.200±0.019 | 0.330±0.0251 |

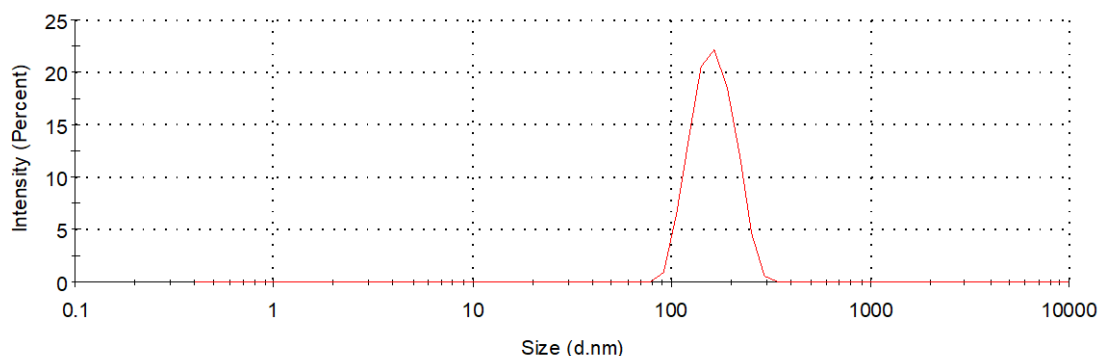


Figure (11): Hydrodynamic size distribution of the dapsona nanocrystal after storage for three months.

3.12. *In vitro* anti-inflammatory activity of dapsona

3.12.1. Inhibition of albumin denaturation.

Dapsona nanocrystal (F2) produced 8.76% inhibition of albumin denaturation percentage starting from the lowest used concentration (50 $\mu\text{g/mL}$). The highest inhibition percent, 61.09%, was obtained upon using 500 $\mu\text{g/mL}$ of DPS-NC (figure 12). All the used concentrations of DPS-NC showed inhibition of albumin denaturation while the pure drug showed inhibition only starting from a concentration equal to 300 $\mu\text{g/mL}$ or higher whereas the pure drug produced only 24.23% inhibition of albumin denaturation at 500 $\mu\text{g/mL}$ as presented in figure 12. The enhanced albumin denaturation of DPS-NC compared to pure could be attributed to the higher solubility of nanocrystal as presented in figure 4. Moreover, the inhibition of albumin denaturation of Span coated DPS-NC was a concentration dependent which means increasing the soluble drug concentration at the affected sites or tissues will result in greater protection of tissues and organs against inflammation and rapid pain relief (Devi et al. 2022).

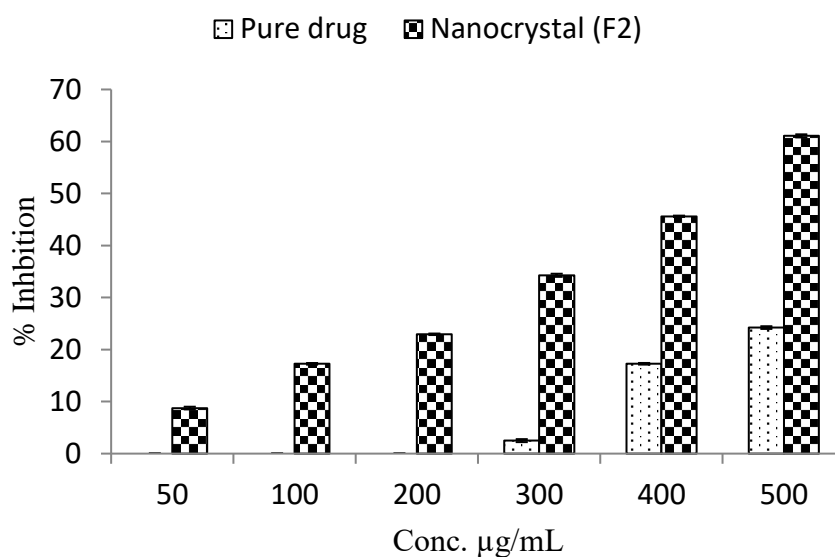


Figure (12): Effect of pure dapsone and dapsone nanocrystal on egg albumin denaturation

3.12.2. Human red blood cell (HRBC) membrane stabilization methods.

Hypotonic solution and heat are considered injurious agents that can lead to lysis of RBCs membrane which is the first step in the inflammation mechanism. So stabilization of RBCs membrane is a standard measure of the anti-inflammatory activity because it prevents the extracellular release of lysosomal constituents of activated leukocytes (such as proteases enzymes), which causes tissue inflammation and might be ended by tissue damage (Rashid et al. 2011).

3.12.3. Heat-induced hemolysis:

Dapsone nanocrystal showed inhibition of RBCs hemolysis starting from the lowest used concentration, 50 $\mu\text{g/mL}$, which gave 23.6% inhibition. The highest inhibition percent, 67.4%, was obtained upon using 500 $\mu\text{g/mL}$. All the applied concentrations of dapsone NC showed inhibition of RBCs hemolysis while pure dapsone showed inhibition starting from 100 $\mu\text{g/mL}$ or higher. The enhanced protection of RBCs hemolysis of NC compared to the pure drug could be attributed to the higher solubility of NC as figure 13. Moreover, the inhibition of RBCs hemolysis of Span coated NC was a concentration-dependent manner which was considered the main parameter in tissue protection against inflammation and relief pain. The present study showed that at a concentration of 50 $\mu\text{g/mL}$ pure drug does not show any inhibition while nanocrystals show 23.6% inhibition using the same concentration. The maximum percentage of inhibition 67.4 % was obtained by using 500 $\mu\text{g/mL}$ concentration for nanocrystals in comparison to only 32.87 % inhibition of pure drug at the same concentration (Aidoo et al. 2021).

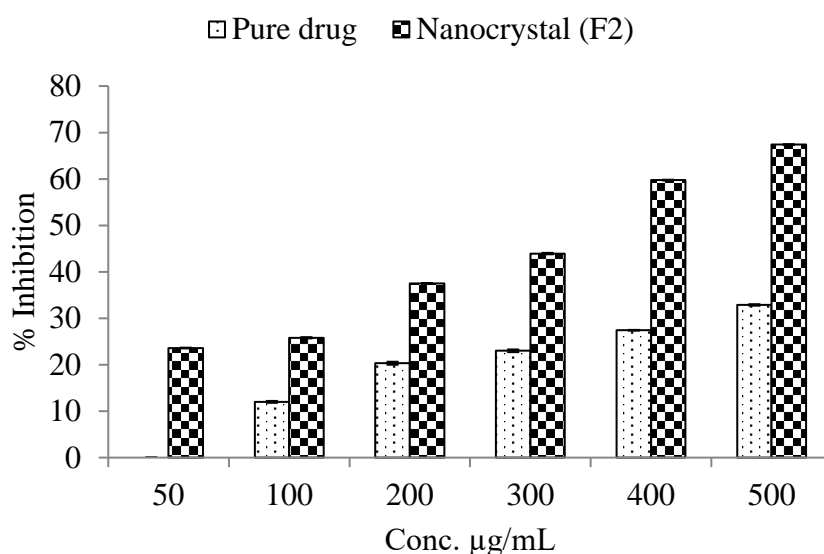


Figure (13): Effect of pure dapsone and dapsone nanocrystal on hemolysis of RBCs induced by heat.

3.12.4. Hypotonicity-induced hemolysis

Hypotonicity means excessive accumulation of fluid into the cells resulting in rupture of the RBCs membrane and cells hemolysis which is followed by leakage of hemoglobin which could be prevented by membrane stabilization. 50 $\mu\text{g/mL}$ of dapsone nanocrystals produce 35.24 % inhibition of RBCs hemolysis. The highest hemolysis inhibition percent, 60.27%, was obtained with 500 $\mu\text{g/mL}$. All the tested concentrations of NC showed inhibition of RBCs hemolysis while the pure drug concentration showed only inhibition at 200 $\mu\text{g/ mL}$ or higher. The enhancement of NC compared to pure could be attributed to sufficient higher solubility of NC as in figure 14. Moreover, the inhibition of RBCs hemolysis of Span stabilized DPS-NC is a concentration-dependent manner which was considered the main parameter in tissue protection against inflammation and relief of pain. At a minimally used concentration, 50 $\mu\text{g/mL}$, the pure drug did not show any inhibition while nanocrystals show 35.24% at the same concentration level and a maximum percentage of inhibition of 60.27% was obtained at 500 $\mu\text{g/mL}$ concentration for nanocrystals in comparison to only 37.11% of pure drug at the same concentration (Gudimella et al. 2022).

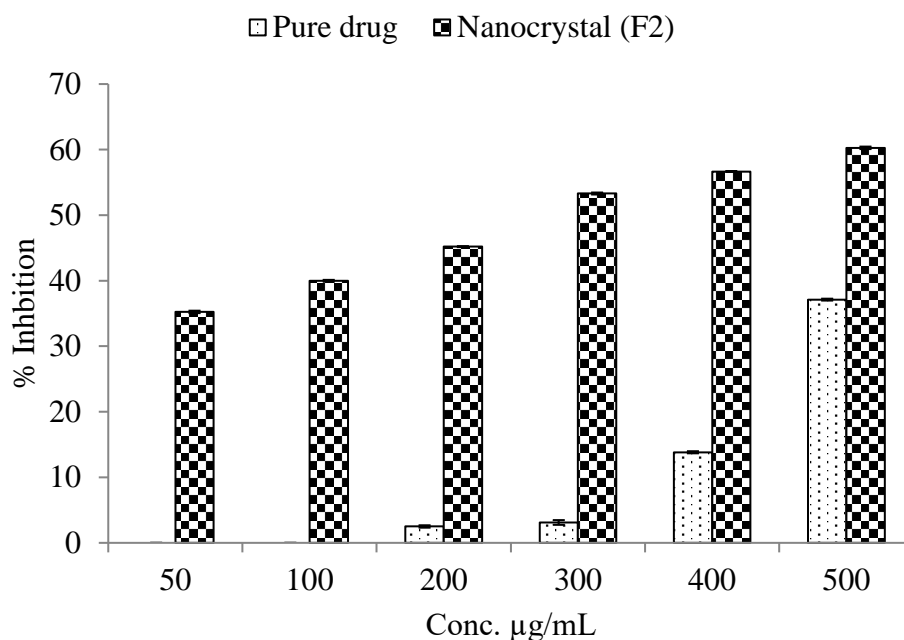


Figure (14): Effect of pure dapsone and dapsone nanocrystal on hemolysis of RBCs induced by hypotonicity.

4. Discussion

Enhancement the solubility and the dissolution rate of hydrophobic drugs are essential preformulation steps toward the development of therapeutically effective dosage forms (Savjani and et al. 2012). In the current study, the improved aqueous saturated solubility of DPS-NC, relative to that of pure drug, was attributed to the decreased particle size and increased surface area in addition to the presence of Span on the particles surface. Generally, aqueous saturation solubility is inversely proportional to particle size i.e the solubility in water increases with decreasing particle size. It is expected also that, nanocrystallization and Span coating could also enhance the dissolution and improve the bioavailability of highly water insoluble dapsone as a BCS class II drug (Dora et al. 2010; Schneider-Rauber, Argenta, and Caon 2020).

Hydrophilic surface active agents and polymers are widely used to stabilize the nanoform of drugs and active pharmaceutical ingredients due to steric stabilization and formation of hydrophilic coat into the particle surfaces. However, Spans (lipophilic surfactant) are not commonly used as a surface coat for nanoparticles intended for drug delivery applications. It is widely used for stabilization of vesicular-based drug delivery system such as liposomes, niosomes and proniosomes (Minamisakamoto et al. 2021; Altamimi et al. 2021). The manipulation of the highly lipophilic dapsone nanocrystal surfaces with a Span 80, relatively more hydrophilic coat, resulted in increased aqueous wettability of the produced nanocrystal. Span was effective in producing stable nanocrystal dispersions of the highly hydrophobic drug, dapsone, due to its high affinity and to the particle surfaces. The hydrophobic part of Span is larger than the hydrophilic part and hence molecules of such structure oriented themselves where the larger

hydrophobic part directed toward the lyophobic surfaces of the particles and the smaller hydrophilic part directed toward the aqueous dispersion medium. The effect of Span 80, as surface stabilizer, was predominant in preparation of small highly water dispersible dapsona nanocrystals. Moreover, the surface charges (zeta potentials) of the produced nanocrystals were between -19.1 mV to -39.6 mV which is sufficient enough to stabilize the obtained nanocrystals. We can conclude that, Span coated dapsona nanoparticles are stabilized by steric stabilization due to presence of Span 80 corona around nanocrystal core and electrostatic repulsion between similarly charged particles due to high negative zeta potential values (**Hayashi et al. 2011; Lowry et al. 2016**).

Dapsona/Span ratios played an important role in the production of stable water dispersible dapsona nanocrystals. Several drug/surfactant ratios were applied for the preparation of DPS-NCs using varying amounts (25, 45, and 65 mg) of Span 80 to varying amounts of the drug (100, 75, and 50 mg) as presented in table 1. Generally, it was found that as the drug to Span 80 ratio increases the size of the produced DPS-NCs increases. The sizes of formulae prepared using 25 mg of Span (F1, F4 and F7) were relatively large. This result may be attributed to used amount of Span 80 (25 mg) was not efficiently to inhibit the crystal growth during the nanocrystal formation and was not enough coated the produced nanocrystals. Among all prepared nanocrystals, these formulae showed the lower values of negative zeta potentials. In contrast, nanocrystals prepared using the low drug/Span ratios (F2, F3, F5, F6, F8 and F9) were having an acceptable particles size range with reasonable zeta potentials (**Zayed and Tessmar 2012**).

High *in vitro* release rate was shown by F2 nanocrystal which is obtained a drug/surfactant ratio of 2.22. This nanocrystal formula was prepared with 45 mg of Span 80 and 100 mg of the drug. The highest *in vitro* release rate of F2 nanocrystal was attributed to the small particle size and coating of the nanocrystal surface with an intermediate amount of the hydrophobic stabilizer. While nanocrystals prepared using the lowest drug/surfactant ratios (F3, F6, and F9) showed the smallest particle sizes of all prepared formulae. These formulae did not show a higher *in vitro* dissolution rate because of the high Span 80 content on the particles surface which delayed the dissolution rates (**Shao et al. 2015; Birdsall and Qing Yu n.d 2018**).

Based on all above mentioned facts and interpretations, several factors should be considered during the nanocrystallization of drugs aiming to enhance drug solubility, dissolution, bioavailability and efficacy. The particle size and size distribution are not only the main factors responsible for enhancing the solubility and therapeutic efficacy but other parameters such as the physicochemical properties of the used stabilizer, surface hydrophilicity, drug/stabilizer ratio, production efficiency, and nanoparticles stability in addition to the intended site of application are also contributing factors for the preparation successful nanoparticles based dosage forms.

Conclusion

Recently, nanocrystallization of poorly water soluble drugs is considered to be effective method for enhancing the drug's aqueous solubility, dissolution rate, and therapeutic efficacy. In this study, a unique Span 80 stabilized dapsona nanocrystal had been successfully prepared and characterized applying solvent anti-solvent crystallization

technique. Span coated DPS-NC was in the nanocrystal range, below 100 nm in diameter, and had a certain degree of crystallinity as indicated by X-ray diffraction and TEM imaging. The engineered nanocrystals possess higher solubility and rapid dissolution rates compared to untreated drug. Additionally, DPS-NCs showed a significant increase in the *in vitro* anti-inflammatory activity. These results could be promising and attractive for the development of DPS-NCs loaded drug delivery system with an enhanced anti-inflammatory. The proposed system will be smart and novel for the effective treatment of infected and inflamed acne at the same time.

Funding Statement

The authors didn't receive any financial support to carry out this work and the work described was funded by the authors themselves. This work was carried out in the Department of Pharmaceutics and Pharmaceutical Technology, Faculty of Pharmacy, Al-Azhar University at Assiut, Egypt.

REFERENCES

- Abid, Namra, Aqib Muhammad Khan, Sara Shujait, Kainat Chaudhary, Muhammad Ikram, Muhammad Imran, Junaid Haider, Maaz Khan, Qasim Khan, and Muhammad Maqbool. 2022.** "Synthesis of Nanomaterials Using Various Top-down and Bottom-up Approaches, Influencing Factors, Advantages, and Disadvantages: A Review." *Advances in Colloid and Interface Science* 300(December):102597. doi: 10.1016/j.cis.2021.102597.
- Agrawal, Shikha, S. S. Pancholi, N. K. Jain, and G. P. Agrawal. 2004.** "Hydrotropic Solubilization of Nimesulide for Parenteral Administration." *International Journal of Pharmaceutics* 274(1–2):149–55. doi: 10.1016/j.ijpharm.2004.01.012.
- Aidoo, Douglas Bosco, Daniels Konja, Isaac Tabiri Henneh, and Martins Ekor. 2021.** "Protective Effect of Bergapten against Human Erythrocyte Hemolysis and Protein Denaturation in Vitro." *International Journal of Inflammation* 2021. doi: 10.1155/2021/1279359.
- Alshweiat, Areen, Gábor Katona, Ildikó Csóka, and Rita Ambrus. 2018.** "Design and Characterization of Loratadine Nanosuspension Prepared by Ultrasonic-Assisted Precipitation." *European Journal of Pharmaceutical Sciences* 122(May):94–104. doi: 10.1016/j.ejps.2018.06.010.
- Alston, Melissa, Glyn Hobbs, and Ismini Nakouti. 2022.** "Acne Vulgaris : The Skin Microbiome , Antibiotics and Whether Natural Products Could Be Considered a Suitable Alternative Treatment ?" 1(1):1–11. doi: 10.24377/jnpd.article652.
- Altamimi, Mohammad A., Afzal Hussain, Mohammad Alrajhi, Sultan Alshehri, Syed Sarim Imam, and Wajhul Qamar. 2021.** "Luteolin-Loaded Elastic Liposomes for Transdermal Delivery to Control Breast Cancer: In Vitro and Ex Vivo Evaluations." *Pharmaceutics* 14(11). doi: 10.3390/ph14111143.

- Altamimi, Mohammad A., and Steven H. Neau. 2016.** “Use of the Flory-Huggins Theory to Predict the Solubility of Nifedipine and Sulfamethoxazole in the Triblock, Graft Copolymer Soluplus.” *Drug Development and Industrial Pharmacy* 42(3):446–55. doi: 10.3109/03639045.2015.1075033.
- Alves, Helton José, Lázaro José Gasparrini, Felipe Eduardo, Bueno Silva, Laressa Caciato, Graciela Ines, Bolzon De Muniz, Eduardo Luis, Cupertino Ballester, Paulo André Cremonez, and Mabel Karina Arantes. 2021.** “Alternative Methods for the Pilot-Scale Production and Characterization of Chitosan Nanoparticles.” 10977–87.
- Ashok Kumar, J., S. Ramkanth, S. Lakshmana Prabu, and V. Gopal. 2015.** “Enhancement of Saturation Solubility and In Vitro Dissolution of Carvedilol Nanoparticles by High Pressure Homogenization Technique.” *International Journal of Current Pharmaceutical Review and Research* 6(6):269–73.
- Bailey-shaw, Yvonne A., Lawrence A. D. Williams, Cheryl E. Green, Shawntae Rodney, and Ann Marie Smith. 2017.** “In-Vitro Evaluation of the Anti-Inflammatory Potential of Selected Jamaican Plant Extracts Using the Bovine Serum Albumin Protein Denaturation Assay.” *International Journal of Pharmaceutical Sciences Review and Research* 47(1):145–53.
- Bawazeer, Saud, Dalia Farag A. El-Telbany, Majid Mohammad Al-Sawahli, Gamal Zayed, Ahmed Abdallah A. Keed, Abdelaziz E. Abdelaziz, and Doaa H. Abdel-Naby. 2020.** “Effect of Nanostructured Lipid Carriers on Transdermal Delivery of Tenoxicam in Irradiated Rats.” *Drug Delivery* 27(1):1218–30. doi: 10.1080/10717544.2020.1803448.
- Bergström, Christel A. S., Sara B. E. Andersson, Jonas H. Fagerberg, Gert Ragnarsson, and Anders Lindahl. 2014.** “Is the Full Potential of the Biopharmaceutics Classification System Reached?” *European Journal of Pharmaceutical Sciences* 57(1):224–31. doi: 10.1016/j.ejps.2013.09.010.
- Berson, Diane S., and Alan R. Shalita. 1995.** “The Treatment of Acne: The Role of Combination Therapies.” *Journal of the American Academy of Dermatology* 32(5 PART 3). doi: 10.1016/0190-9622(95)90418-2.
- Birdsall, Robert E., and Ying Qing Yu. n.d. 2018** “An Efficient UV-Based Method for the Assessment of Oleic Acid Content in Biotherapeutic Drug Products Containing Polysorbate-80.” 1–8. February.
- Brown, Patricia, and Food And Drug Administration. 2014.** “ACZONE Clinical Review.” 22–129.
- Chaves, Luíse L., Alexandre C. C. Vieira, Domingos Ferreira, Bruno Sarmiento, and Salette Reis. 2015.** “Rational and Precise Development of Amorphous Polymeric Systems with Dapsone by Response Surface Methodology.” *International Journal of Biological Macromolecules* 81:662–71. doi:

10.1016/j.ijbiomac.2015.08.009.

- Chen, Huabing, Chalermchai Khemtong, Xiangliang Yang, Xueling Chang, and Jinming Gao. 2011.** “Nanonization Strategies for Poorly Water-Soluble Drugs.” *Drug Discovery Today* 16(7–8):354–60. doi: 10.1016/j.drudis.2010.02.009.
- Devi, Sunita, Sunil Kumar, Vikas Verma, Deepak Kaushik, Ravinder Verma, and Meenakshi Bhatia. 2022.** “Enhancement of Ketoprofen Dissolution Rate by the Lquisolid Technique: Optimization and in Vitro and in Vivo Investigations.” *Drug Delivery and Translational Research* (0123456789). doi: 10.1007/s13346-022-01120-x.
- Dora, Chander Parkash, Shailendra Kumar Singh, Sanjeev Kumar, Ashok Kumar Datusalia, and Aakash Deep. 2010.** “Development and Characterization of Nanoparticles of Glibenclamide by Solvent Displacement Method.” *Acta Poloniae Pharmaceutica - Drug Research* 67(3):283–90.
- El-Feky, Gina S., Gamal Zayed, and Abdel Razik H. Farrag. 2013.** “Optimization of an Ocular Nanosuspension Formulation for Acyclovir Using Factorial Design.” *International Journal of Pharmacy and Pharmaceutical Sciences* 5(SUPPL.1): 213–19.
- Gao, Lei, Guiyang Liu, Jianli Ma, Xiaoqing Wang, Liang Zhou, and Xiang Li. 2012.** “Drug Nanocrystals: In Vivo Performances.” *Journal of Controlled Release* 160(3):418–30. doi: 10.1016/j.jconrel.2012.03.013.
- Gudimella, Krishna kanthi, Gangaraju Gedda, P. Senthil Kumar, B. K. Babu, Bhaskar Yamajala, Battula Venkateswara Rao, Prabal Pratap Singh, Deepak Kumar, and Ajit Sharma. 2022.** “Novel Synthesis of Fluorescent Carbon Dots from Bio-Based Carica Papaya Leaves: Optical and Structural Properties with Antioxidant and Anti-Inflammatory Activities.” *Environmental Research* 204(PA):111854. doi: 10.1016/j.envres.2021.111854.
- Gunathilake, K. D. P. P., K. K. D. S. Ranaweera, and H. P.V. Rupasinghe. 2018.** “Influence of Boiling, Steaming and Frying of Selected Leafy Vegetables on the in Vitro Anti-Inflammation Associated Biological Activities.” *Plants* 7(1). doi: 10.3390/plants7010022.
- Gunathilake, K. D. P. P., K. K. D. S. Ranaweera, and H. P.Vasantha Rupasinghe. 2018.** “In Vitro Anti-Inflammatory Properties of Selected Green Leafy Vegetables.” *Biomedicines* 6(4):1–10. doi: 10.3390/biomedicines6040107.
- Hayashi, Keita, Toshinori Shimanouchi, Keiichi Kato, Tatsuhiko Miyazaki, Atsushi Nakamura, and Hiroshi Umakoshi. 2011.** “Span 80 Vesicles Have a More Fluid, Flexible and ‘Wet’ Surface than Phospholipid Liposomes.” *Colloids and Surfaces B: Biointerfaces* 87(1):28–35. doi: 10.1016/j.colsurfb.2011.04.029.
- He, Jiali, Yue Han, Gujun Xu, Lifang Yin, M. Ngandeu Neubi, Jianping Zhou, and**

- Yang Ding. 2017.** “Preparation and Evaluation of Celecoxib Nanosuspensions for Bioavailability Enhancement.” *RSC Advances* 7(22):13053–64. doi: 10.1039/c6ra28676c.
- Ibrahim, Mohamed A., Gamal M. Zayed, Fahd M. Alsharif, and Wael A. Abdelhafez. 2019.** “Utilizing Mixer Torque Rheometer in the Prediction of Optimal Wet Massing Parameters for Pellet Formulation by Extrusion/Spheronization.” *Saudi Pharmaceutical Journal* 27(2):182–90. doi: 10.1016/j.jpsps.2018.10.002.
- Junyaprasert, Varaporn Buraphacheep, and Boontida Morakul. 2015.** “Nanocrystals for Enhancement of Oral Bioavailability of Poorly Water-Soluble Drugs.” *Asian Journal of Pharmaceutical Sciences* 10(1):13–23. doi: 10.1016/j.ajps.2014.08.005.
- Khan, Ajmal, Umar Farooq, Touqeer Ahmad, Rizwana Sarwar, Jazib Shafiq, Yasir Raza, Ayaz Ahmed, Safi Ullah, Najeeb Ur Rehman, and Ahmed Al-Harrasi. 2019.** “Rifampicin Conjugated Silver Nanoparticles: A New Arena for Development of Antibiofilm Potential against Methicillin Resistant Staphylococcus Aureus and Klebsiella Pneumonia.” *International Journal of Nanomedicine* 14:3983–93. doi: 10.2147/IJN.S198194.
- Khan, Jahangir, Sajid Bashir, Muhammad Asif Khan, Attiq Naz, Rukhsana Ghaffar, Shujaat Ahmad, Abid Ullah, Kifayat Ullah Shah, Nauman Rahim Khan, and Mohammad Isreb. 2020.** “Smart Nanocrystal of Indomethacin: Nanonization and Characterization through Top down Method of Media Milling.” *Pakistan Journal of Pharmaceutical Sciences* 33(2):765–70.
- Li, Wanya, Yiming Ma, Yang Yang, Shijie Xu, Peng Shi, and Songgu Wu. 2019.** “Solubility Measurement, Correlation and Mixing Thermodynamics Properties of Dapsone in Twelve Mono Solvents.” *Journal of Molecular Liquids* 280:175–81. doi: 10.1016/j.molliq.2019.02.023.
- Lowry, Gregory V., Reghan J. Hill, Stacey Harper, Alan F. Rawle, Christine Ogilvie Hendren, Fred Klaessig, Ulf Nobbmann, Philip Sayre, and John Rumble. 2016.** “Guidance to Improve the Scientific Value of Zeta-Potential Measurements in NanoEHS.” *Environmental Science: Nano* 3(5):953–65. doi: 10.1039/c6en00136j.
- Medarević, Djordje, Svetlana Ibrić, Elisavet Vardaka, Miodrag Mitrić, Ioannis Nikolakakis, and Kyriakos Kachrimanis. 2020.** “Insight into the Formation of Glimepiride Nanocrystals by Wet Media Milling.” *Pharmaceutics* 12(1). doi: 10.3390/pharmaceutics12010053.
- Merisko-Liversidge, Elaine M., and Gary G. Liversidge. 2008.** “Drug Nanoparticles: Formulating Poorly Water-Soluble Compounds.” *Toxicologic Pathology* 36(1):43–48. doi: 10.1177/0192623307310946.

- Minamisakamoto, Takaya, Shuhei Nishiguchi, Kazuki Hashimoto, Ken ichi Ogawara, Masato Maruyama, and Kazutaka Higaki. 2021.** “Sequential Administration of PEG-Span 80 Niosome Enhances Anti-Tumor Effect of Doxorubicin-Containing PEG Liposome.” *European Journal of Pharmaceutics and Biopharmaceutics* 169(August):20–28. doi: 10.1016/j.ejpb.2021.08.013.
- Mosharraf, Mitra, and Christer Nyström. 1995.** “The Effect of Particle Size and Shape on the Surface Specific Dissolution Rate of Microsized Practically Insoluble Drugs.” *International Journal of Pharmaceutics* 122(1–2):35–47. doi: 10.1016/0378-5173(95)00033-F.
- Mothilal, M., M. Chaitanya Krishna, S. P. Surya Teja, V. Manimaran, and N. Damodharan. 2014.** “Formulation and Evaluation of Naproxen-Eudragit ® RS 100 Nanosuspension Using 32 Factorial Design FORMULATION AND EVALUATION OF NAPROXEN-EUDRAGIT ® RS 100 NANOSUSPENSION USING 3 2 FACTORIAL DESIGN.” (January).
- Nyamba, Isaïe, Anna Lechanteur, Rasmané Semdé, and Brigitte Evrard. 2021.** “Physical Formulation Approaches for Improving Aqueous Solubility and Bioavailability of Ellagic Acid: A Review.” *European Journal of Pharmaceutics and Biopharmaceutics* 159:198–210. doi: 10.1016/j.ejpb.2020.11.004.
- Rashid, Mohammad A., Md Al Amin Sikder, Mohammad A. Kaiser, Md Kowser Miah, Md Masud Parvez, Akm Nawshad Hossian, and Mohammad Abdur Rashid. 2011.** “Membrane Stabilizing Activity-a Possible Mechanism of Action for the Anti-Inflammatory Activity of Two Bangladeshi Medicinal Plants: Mesua Nagassarium (Burm.F.) and Kigelia Pinnata (Jack) Dc.” *International Standard Serial Number* 3(3):1–5.
- Saso, Luciano, Giovanni Valentini, Maria Luisa Casini, Eleonora Grippa, Maria Teresa Gatto, Maria Grazia Leone, and Bruno Suvestrini. 2001.** “Inhibition of Heat-Induced Denaturation of Albumin by Nonsteroidal Antiinflammatory Drugs (NSAIDs): Pharmacological Implications.” 24(2):150–58.
- Savjani, Ketan T., Anuradha K. Gajjar, and Jignasa K. Savjani. 2012.** “Drug Solubility: Importance and Enhancement Techniques.” *ISRN Pharmaceutics* 2012(100 mL):1–10. doi: 10.5402/2012/195727.
- Schneider-Rauber, Gabriela, Debora Fretes Argenta, and Thiago Caon. 2020.** “Emerging Technologies to Target Drug Delivery to the Skin – the Role of Crystals and Carrier-Based Systems in the Case Study of Dapsone.” *Pharmaceutical Research* 37(12):6–10. doi: 10.1007/s11095-020-02951-4.
- Shalita, Alan R., James Q. Del Rosso, and Guy F. Webster. 2011.** “Acne Vulgaris.” *Acne Vulgaris* 1–228. doi: 10.29309/tpmj/2013.20.03.901.
- Shao, Xiao Ru, Xue Qin Wei, Xu Song, Li Ying Hao, Xiao Xiao Cai, Zhi Rong Zhang, Qiang Peng, and Yun Feng Lin. 2015.** “Independent Effect of Polymeric

Nanoparticle Zeta Potential/Surface Charge, on Their Cytotoxicity and Affinity to Cells.” *Cell Proliferation* 48(4):465–74. doi: 10.1111/cpr.12192.

- Shariare, Mohammad H., S. Sharmin, I. Jahan, H. M. Reza, and Kazi Mohsin. 2018.** “The Impact of Process Parameters on Carrier Free Paracetamol Nanosuspension Prepared Using Different Stabilizers by Antisolvent Precipitation Method.” *Journal of Drug Delivery Science and Technology* 43(October 2017):122–28. doi: 10.1016/j.jddst.2017.10.001.
- Sinha, Biswadip, Rainer H. Müller, and Jan P. Möschwitzer. 2022.** “Bottom-up Approaches for Preparing Drug Nanocrystals: Formulations and Factors Affecting Particle Size.” *International Journal of Pharmaceutics* (January 2013). doi: 10.1016/j.ijpharm.2013.01.019.
- Toyoda, Masahiko, and M. Morohashi. 2001.** “Pathogenesis of Acne.” *Medical Electron Microscopy* 34(1):29–40. doi: 10.1007/s007950100002.
- Umapathy, E., E. J. Ndebia, A. Meeme, B. Adam, P. Menziwa, B. N. Nkeh-Chungag, and J. E. Iputo. 2010.** “An Experimental Evaluation of *Albuca Setosa* Aqueous Extract on Membrane Stabilization, Protein Denaturation and White Blood Cell Migration during Acute Inflammation.” *Journal of Medicinal Plants Research* 4(9):789–95. doi: 10.5897/JMPR10.056.
- Wang, Yancai, Ying Zheng, Ling Zhang, Qiwei Wang, and Dianrui Zhang. 2013.** “Stability of Nanosuspensions in Drug Delivery.” *Journal of Controlled Release* 172(3):1126–41. doi: 10.1016/j.jconrel.2013.08.006.
- Wozel, Gottfried, and Christian Blasum. 2014.** “Dapsone in Dermatology and Beyond.” *Archives of Dermatological Research* 306(2):103–24. doi: 10.1007/s00403-013-1409-7.
- Xiao, Shanshan, Hang Yu, Yunfei Xie, Yahui Guo, Jiajia Fan, and Weirong Yao. 2021.** “The Anti-Inflammatory Potential of *Cinnamomum Camphora* (L.) J.Presl Essential Oil in Vitro and in Vivo.” *Journal of Ethnopharmacology* 267:113516. doi: 10.1016/j.jep.2020.113516.
- Xu, Haoxiang, and Huiying Li. 2019.** “Acne, the Skin Microbiome, and Antibiotic Treatment.” *American Journal of Clinical Dermatology* 20(3):335–44. doi: 10.1007/s40257-018-00417-3.
- Zayed, Gamal. 2014.** “Dissolution Rate Enhancement of Ketoprofen By Surface Solid Dispersion With Colloidal Silicon Dioxide.” *Unique Journal of Pharmaceutical and Biological Sciences* 02(01):33–38.
- Zayed, Gamal M. S., and Joerg K. V. Tessmar. 2012.** “Heterobifunctional Poly(Ethylene Glycol) Derivatives for the Surface Modification of Gold Nanoparticles Toward Bone Mineral Targeting.” *Macromolecular Bioscience* 12(8):1124–36. doi: 10.1002/mabi.201200046.

Zhao, Xiuhua, Weiguo Wang, Yuangang Zu, Ying Zhang, Yong Li, Wei Sun, Chang Shan, and Yunlong Ge. 2014. "Preparation and Characterization of Betulin Nanoparticles for Oral Hypoglycemic Drug by Antisolvent Precipitation." *Drug Delivery* 21(6):467–79. doi: 10.3109/10717544.2014.881438.

كريستالات الدابسون النانومترية: نهج جديد لتعزيز الذوبانية ومعدل الذوبان والنشاط المضاد للألتهابات في المختبر

هناء محمد مصطفى¹ - شعبان خلف عبد الحميد² - وجمال محمد سلطان زايد³

¹صيدلانية بمستشفى طب الأزهر الجامعي - جامعة الأزهر فرع أسيوط

²قسم الصيدلانيات والتقنية الصيدلانية - كلية الصيدلة جامعة الأزهر فرع أسيوط

³مركز الأزهر لعلوم النانو وتطبيقاتها - جامعة الأزهر فرع أسيوط

البريد الإلكتروني للباحث الرئيسي : gamalzayed@azhar.edu.eg

أن الذوبانية المنخفضة لعقار الدابسون (دواء يستخدم في علاج حب الشباب) في الماء تحد بشكل كبير من فعاليته البيولوجية وخاصة تأثيره المضاد للالتهاب. في هذه الدراسة تم استخدام تقنية التبلور النانومترية لزيادة مساحة سطح الجسيمات مما يحسن من الذوبانية ومعدل الذوبان في الماء والذي يتبعه تحسن في التأثير المضاد للالتهاب. تم تحضير بلورات الدابسون النانومترية باستخدام تقنية التبلور من مذيب - مضاد المذيب باستخدام الأسيتون كمذيب والماء كمضاد مذيب. تم توصيف البلورات النانومترية بواسطة التحليل الطيفي بالأشعة تحت الحمراء والتحليل الحراري التفاضلي والأشعة السينية. كما تم فحص حجم وشكل وسطح وشحنة السطح للجسيمات بواسطة جهاز زيتاسيزر والمجهر الإلكتروني عالي الكفاءة والمجهر الإلكتروني الماسح. بالإضافة إلى ذلك تم التحقق من قابلية الذوبان والتأثير المضاد للالتهاب للجسيمات المنتجة في المختبر. أوضحت النتائج أن بلورات الدابسون النانومترية المنتجة كروية الشكل، ذات أسطح ملساء ولها حجم هيدروديناميكي يبلغ حوالي 149 نانومتر. كما بينت النتائج أن الذوبان المائي المشبع للجسيمات قد ارتفع بحوالي 6 أضعاف مقارنة بالدواء الخام وأظهرت كذلك تحسناً كبيراً في معدل الذوبان. أثبتت نتائج التحليل الطيفي بالأشعة تحت الحمراء والتحليل الحراري أن السواغات المستخدمة في تحضير الجسيمات لم تتفاعل كيميائياً مع العقار. أكد حيود الأشعة السينية والتصوير بالمجهر الإلكتروني عالي الكفاءة أن البلورات النانومترية التي تم الحصول عليها لا تزال تتمتع بدرجة معينة من التبلور ولم تتحول تماماً إلى الحالة غير المتبلورة. وكذلك تحسن التأثير المضاد للتهاب لبلورات الدابسون النانومترية بشكل كبير مقارنة بالعقار الخام. بناءً على ما سبق، يمكن اعتبار بلورات الدابسون النانومترية خياراً علاجياً جديداً وواعداً وفعالاً لعلاج حب الشباب بالإضافة إلى تخفيف الالتهاب المصاحب له.

الكلمات المفتاحية: دابسون نانوكريستال، مذيب - مضاد للذوبان، الذوبان المشبع، معدل الذوبان، التأثير المضاد للالتهاب في المختبر.